Plerixafor Biases CXCR4 Signaling Through β-Arrestin to Promote Melanogenesis via β-Catenin–MITF Activation

Tsong-Min Chang , Ting-Ya Yang , Huey-Chun Huang *

Posted Date: 23 March 2026

doi: 10.20944/preprints202603.1777.v1

Keywords: CXCR4; β-arrestin; β-catenin; MITF; plerixafor; repigmentation

 doi:10.20944/preprints202603.1777.v1

Article

Plerixafor Biases CXCR4 Signaling Through β-Arrestin to Promote Melanogenesis via β-Catenin–MITF Activation

Tsong-Min Chang [1], Ting-Ya Yang [2] and Huey-Chun Huang [2,*]

[1] Department of Applied Cosmetology, Hungkuang University

[2] Department of Medical Laboratory Science and Biotechnology, College of Medicine, China Medical University

* Correspondence: lchuang@mail.cmu.edu.tw; Tel.: +886-4-22053366 Ext. 7207

Abstract

Plerixafor is a clinically approved CXCR4 antagonist that mobilizes hematopoietic stem cells by disrupting CXCL12/CXCR4 retention signaling. However, its biochemical effects on melanocytes and pigmentation remain unexplored. We investigated how plerixafor modulates CXCR4 signaling in melanocytes and evaluated its potential as a pro-melanogenic agent using in vitro and in vivo approaches. Human PIG1 melanocytes were treated with plerixafor (1–10 nM) with or without hydroquinone, followed by qPCR for MITF and tyrosinase expression, flow cytometry for CXCR4/CXCR7 and integrin profiling, Transwell migration assays, β-arrestin siRNA knockdown, Western blotting, subcellular fractionation, and ChIP-qPCR for β-catenin binding to MITF regulatory regions. A murine HQ-induced depigmentation model was used to test topical plerixafor (0.1–10 mM) on pigmentation, hair follicles, melanogenic gene expression, and systemic safety markers. Plerixafor significantly increased MITF and tyrosinase mRNA and enhanced melanocyte migration, while counteracting HQ-induced suppression of melanogenic genes. Plerixafor reduced cell-surface CXCR4 (consistent with β-arrestin–mediated receptor internalization) without altering CXCR7, c-KIT, or N-cadherin. β-Arrestin knockdown abolished plerixafor-induced ERK phosphorylation and melanogenic responses, confirming β-arrestin dependence. Plerixafor promoted β-catenin nuclear translocation and direct β-catenin occupancy at MITF promoter/enhancer TCF/LEF motifs (5- to 8-fold enrichment, $p<0.05$). In vivo, topical plerixafor restored HQ-induced depigmentation, increased hair follicle number and melanin content, and upregulated cutaneous MITF and tyrosinase without hepatic, renal, or inflammatory toxicity. Plerixafor functions as a biased CXCR4 ligand in melanocytes, engaging a β-arrestin–β-catenin–MITF signaling axis to drive melanogenesis and repigmentation. These findings identify CXCR4 biased antagonism as a tractable pharmacologic strategy for therapeutic repigmentation in pigmentary disorders.

Keywords: CXCR4; β-arrestin; β-catenin; MITF; plerixafor; repigmentation

1. Introduction

The fully differentiated human melanocyte, mainly found in the basal layer of the skin's epidermis, is essential in this layer by producing melanin within its organelles and transferring these pigment-filled organelles to neighboring keratinocytes. Melanocytes respond to various signals, including UV radiation, hormones, and paracrine signaling from surrounding tissues, to control the amount and type of melanin produced [1]. Dysregulation of these factors can lead to pigmentation disorders which melanocytes are lost or dysfunctional. Research indicates that melanocytes are primarily located in reservoirs, particularly within hair follicles. However, the number of functional melanocytes and the ability to produce melanin tend to decrease with age. This decline contributes to the lightening of skin and hair color observed in older individuals [2]. Current treatments for

 doi:10.20944/preprints202603.1777.v1

pigmentation disorders often involve skin grafting or cell therapy using autologous melanocytes. However, these methods are limited by the poor proliferative ability of melanocytes obtained from skin biopsies. Recent advances in generating melanocytes from human pluripotent stem cells have demonstrated potential, providing a more sustainable source for cell therapy [3,4]. Promoting the generation of healthy melanocytes would likely involve enhancing or mimicking the signals that attract and support melanoblast/melanocyte survival and differentiation, which could potentially involve controlled manipulation of chemokine signaling [5]. Understanding the biochemical mechanisms by which CXCR4 antagonists modulate cellular phenotypes beyond stem cell mobilization may reveal novel therapeutic applications. Biased GPCR ligands that selectively activate β-arrestin pathways while blocking G-protein signaling represent a pharmacologically distinct mode of action with tissue-specific consequences that remain incompletely characterized in melanocytes.

Plerixafor (Mozobil®, AMD3100) is a medication primarily used in medicine to mobilize hematopoietic stem cells (HSCs) [6]. It blocks the binding of stromal cell-derived factor-1α (SDF-1α, also known as CXCL12) to CXCR4 [7,8]. This disruption leads to the mobilization or release of these cells from their niche into the peripheral circulation, resulting in their release and subsequent vulnerability to external factors. The CXCL12/CXCR4 signaling axis acts as a primary homing and retention signal. CXCL12 signals primarily through two receptors: CXCR4 and CXCR7. Both are G protein-coupled transmembrane receptors, but they differ in their signaling mechanisms and physiological roles[9]. Pleiotropic effects of the CXCR4/CXCR7/CXCR12 pathway have been reported in various physiopathological processes, as well as in malignant diseases [10,11]. Plerixafor is considered a biased antagonist of the CXCR4 receptor. It effectively blocks the binding of CXCL12 and prevents the activation of the G-protein signaling pathway, which is the canonical pathway responsible for the retention and survival signals within the stem cell niche [12]. Plerixafor also acts as a β-arrestin-biased agonist. Binding to CXCR4 promotes the recruitment of the β-arrestin protein that typically triggers CXCR4 internalization. CXCR7 acts as a decoy receptor, influencing CXCR4 binding to CXCL12 and thereby limiting excessive signaling, which helps maintain the balance between cell movement, survival, and differentiation [13,14].

Our laboratory previously screened a library of 1,500 FDA-approved drugs and unexpectedly discovered that plerixafor promotes melanin production in melanocytes. Studies have revealed its intriguing effects on skin biology and hair follicle dynamics. Treatment with plerixafor protects against the development of UV-induced skin cancer in murine models, highlighting the therapeutic potential of antagonizing this chemokine axis. Plerixafor promotes wound healing in diabetic patients and inhibits tumor proliferation [15–17]. CXCL12 enhances, while plerixafor relieves itch and pain sensations, in the allergic contact dermatitis mouse model [18]. Recently, Zheng et al. identified that silencing the CXCL12/CXCR4 axis stimulates hair growth in androgenetic alopecia [19]. CXCR4 expression in primary melanocytes was variable but consistent[20]. Therefore, we hypothesized that plerixafor acts as a β-arrestin–biased CXCR4 ligand in melanocytes, engaging a β-catenin–MITF transcriptional program to promote melanogenesis and repigmentation. To test this, we combined in vitro pathway dissection in human PIG1 melanocytes with an in vivo hydroquinone-induced depigmentation model to define the CXCR4-dependent mechanisms and therapeutic potential of plerixafor in pigmentation disorders. Hydroquinone (HQ) is a phenolic depigmenting agent that functions primarily as an alternate substrate and competitive inhibitor of tyrosinase, diverting tyrosine oxidation toward non-melanogenic quinones and thereby suppressing melanin synthesis in active melanocytes [21].

2. Results

2.1. Plerixafor Enhanced Melanogenesis

We examined the pro-melanogenic activity of plerixafor by measuring the expression of the key melanogenic regulator MITF at 24 h and tyrosinase at 48 h using qPCR in PIG1 cells. Plerixafor significantly upregulated both MITF and tyrosinase mRNA levels compared with the control group.

 doi:10.20944/preprints202603.1777.v1

These findings suggest that plerixafor stimulates melanogenesis by increasing the transcriptional activity of MITF, which subsequently triggers expression of the tyrosinase gene, thereby increasing melanin production. In contrast, PIG1 cells treated with HQ, which blocks tyrosinase activity and melanogenic genes, showed a reversal of this effect by plerixafor, which might reactivate the MITF/TYR transcriptional program but does not directly relieve tyrosinase inhibition (Figure 1).

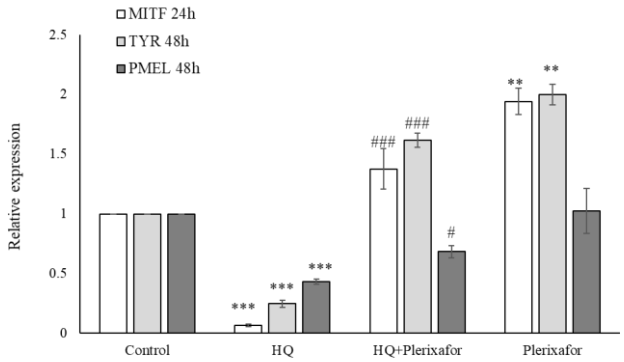

Figure 1. Plerixafor enhances melanogenesis in PIG1 cells. PIG1 cells treated with HQ or plerixafor underwent QPCR using 18S RNA as an internal control. The relative expressions of tyrosinase and MITF were compared to those of the control group. The results are presented as the mean ± SD from at least three independent experiments. P-values are indicated as follows: * $p < 0.05$, ** $p < 0.01$, *** $p < 0.005$ compared to the control.

2.2. Effects of Plerixafor and HQ on PIG1 Cell Migration and Surface Marker Expression

The migration ability in PIG1 cells was enhanced by plerixafor (Figure 2). Surface expression of CXCR4, CXCR7, c-KIT, N-cadherin, and integrin subunits was assessed by flow cytometry with gating based on control MFI. In control PIG1 cells, CXCR4-positive cells constituted approximately 23% of the population. Following plerixafor treatment, the percentage of CXCR4-positive cells decreased significantly to 10% ($p< 0.05$), consistent with receptor internalization [7]. In contrast, the rate of CXCR7-positive cells remained unchanged across treatment groups, indicating that plerixafor selectively modulates CXCR4. (Figure 3A)

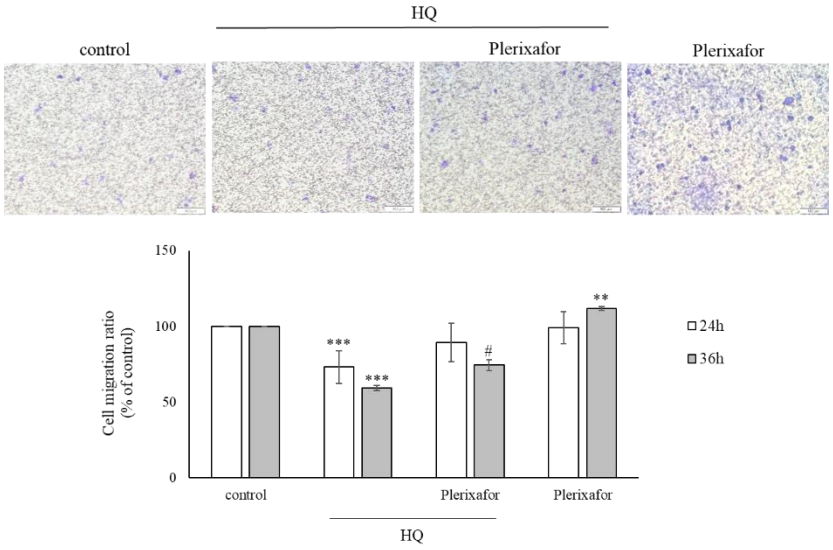

Figure 2. Plerixafor promotes PIG1 cell migration. The trans-well migration measurements were expressed as mean ± SD. Comparisons between multiple groups were conducted using one-way ANOVA.

 doi:10.20944/preprints202603.1777.v1

For melanocyte lineage markers, c-KIT and N-cadherin expression remained stable, with no significant change in % positive cells following HQ or plerixafor treatment (c-KIT: control 37% vs HQ 36% vs plerixafor 36%, $p<0.05$; N-cadherin: control 35% vs HQ 35% vs plerixafor 35%, $p<0.05$).

Integrin profiling revealed that HQ treatment reduced the percentage of integrin β1-positive cells from 48% to 8% ($p<0.05$). Conversely, integrin αv-positive cells increased from 49% to 99% following HQ treatment ($p<0.05$), suggesting a shift in integrin heterodimer composition. Plerixafor did not significantly alter integrin β1 or αv expression compared with HQ-treated cells, indicating that plerixafor-induced migration occurs independently of integrin modulation. (Figure 3B). These results suggest that HQ shifts the balance of integrins β1/αv, which can influence cell motility; however, the actual outcomes depend on how the integrin is reconfigured and the specific composition of the extracellular matrix [22].

3A

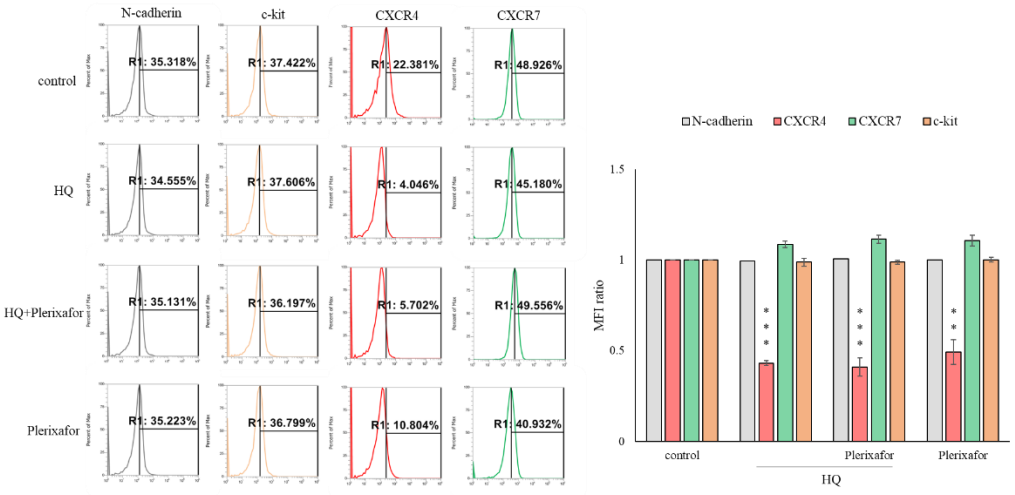

3B

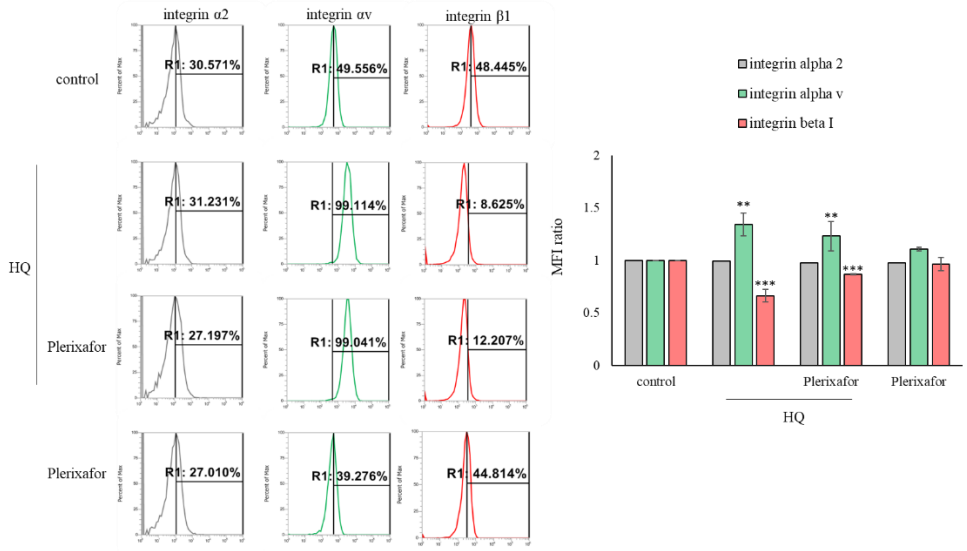

Figure 3. Plerixafor modulates integrin expression and CXCR receptor levels in PIG1 cells. (A) Representative histograms showing fluorescence intensity distributions for CXCR4, CXCR7, c-KIT, and N-cadherin; gray-lined histograms represent vehicle controls. (B) Integrin subunit expression (αv, α2, β1). The right panels show quantification as fold change in MFI relative to controls. Data represent mean ± SD from three independent experiments. Statistical significance: *$p<0.05$, **$p<0.01$, ***$p<0.001$ vs control; #$p<0.05$ vs HQ group.

 doi:10.20944/preprints202603.1777.v1

2.3. Plerixafor Enhances β-Catenin Activation

We further investigated the mechanism in PIG1 cells responding to plerixafor, which blunts CXCR4-driven retention in combination with integrin modulation. Plerixafor exhibits biased antagonism at CXCR4 by selectively blocking G protein–mediated signaling while still promoting β-arrestin recruitment to the receptor. [23,24]. We use siRNA to knock down the level of β-arrestin to dissect pathway specificity in melanocytes in plerixafor signaling. Transfection with si-β-arrestin markedly reduced β-arrestin protein levels, as confirmed by western blotting (Figure 4A). β-arrestin knockdown markedly reduces basal and plerixafor-mediated ERK phosphorylation, indicating that when G-protein signaling is blocked by plerixafor, any residual ERK activity is β-arrestin–dependent Nevertheless, the loss of plerixafor responsiveness in β-arrestin–deficient cells supports a critical role for β-arrestin in this pathway.

Among key transcription factors binding the MITF Promoter, a notable β-catenin translocation was detected in subcellular fractionation, compared with vehicle controls (Figure 4B). To determine the direct association with MITF regulatory sequences, we performed ChIP using anti-β-catenin antibodies, followed by qPCR with primers targeting the MITF promoter/enhancer regions that contain putative TCF/LEF binding motifs. ChIP-qPCR revealed a significant enrichment of β-catenin at these MITF regulatory loci in stimulated cells versus HQ (5- to 8-fold, $p<0.05$), indicating that nuclear β-catenin directly binds to MITF-associated chromatin regions. These data showed that β-catenin translocation to the nucleus enables direct transcriptional regulation of MITF by β-catenin–TCF/LEF complexes, linking signaling to MITF-mediated transcriptional programs (Figure 4C).

4A

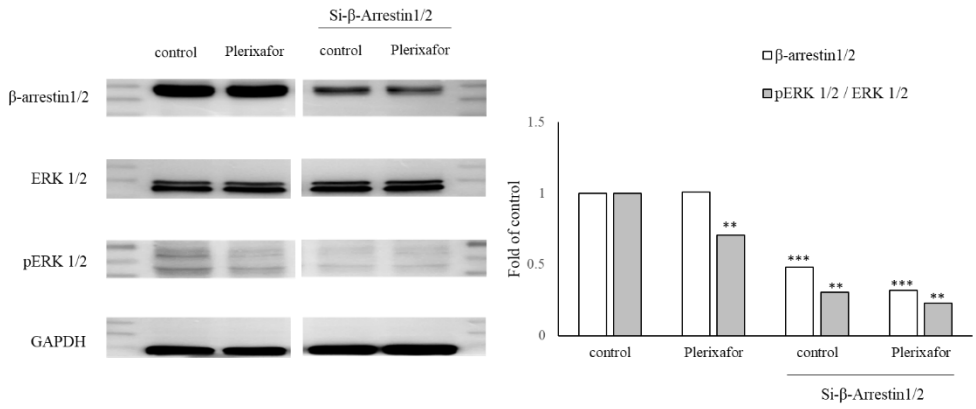

4B

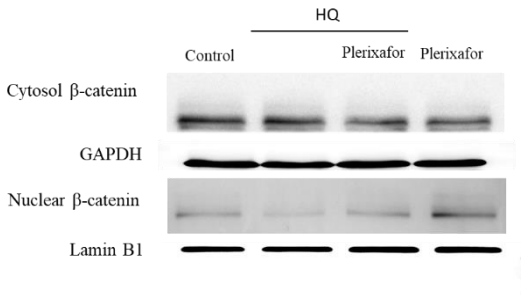

4C

 doi:10.20944/preprints202603.1777.v1

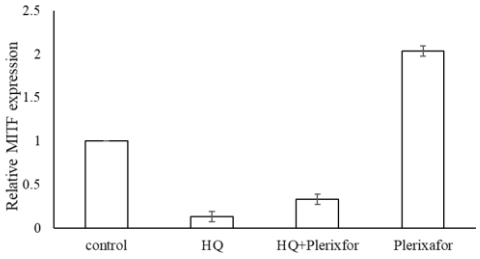

Figure 4. Plerixafor activates the transcriptional interaction between β-catenin and MITF. (A) Representative immunoblot of phosphorylated ERK1/2 (p-ERK) and total ERK1/2 (t-ERK) treated with si-β-arrestin1/2. Densitometric analysis showing the ratio of p-ERK/t-ERK, normalized to control (n=3, mean ± SEM). *p < 0.05, **p < 0.01 vs. control. (B) Western blot analysis reveals the nuclear translocation of β-catenin in PIG1 cells treated with plerixafor. (C) A ChIP-qPCR assay reveals that plerixafor treatment increases the binding of β-catenin to the promoter regions of MITF. The fold enrichment is shown relative to the IgG control. Data are shown as mean ± SD. **P < 0.01, ***P < 0.001 versus the control group.

2.4. Plerixafor Improved Re-Pigmentation in a Mouse Model Treated with HQ

Using HQ caused visible depigmentation on the backs of C57BL/6 mice. Topically applied plerixafor improved repigmentation. Skin tissue analysis and HE staining revealed no local skin irritation or histologic inflammation (Figure 5A). A significant difference in the number of hair follicles was observed between the experimental groups. Fontana-Masson staining was used to visualize and measure melanin, revealing that HQ eliminated hair follicles and their melanin content by approximately 50% compared with controls. In contrast, topical plerixafor treatment restored the eliminated hair follicles, resulting in a 1.5-fold increase in their number and melanin content ($p<0.05$), consistent with restoration of pigment production. (Figure 5B). These structural changes did not differ following concentration variation; it appears that the 0.1 mM topical dose is sufficient to affect melanogenesis and enhance hair follicle regeneration. Biochemical tests revealed that serum AST and creatinine levels remained within normal ranges, confirming that the animal study did not cause liver or kidney damage and did not induce toxicity. The spleen-to-body weight ratio showed no significant difference compared to the control group (Figure 5C). Plerixafor also increased the gene expression of MITF and tyrosinase in skin tissue, as indicated by qPCR analysis (Figure 5D). This in vivo mouse model therefore further supports a pro-melanogenic role for plerixafor.

5A

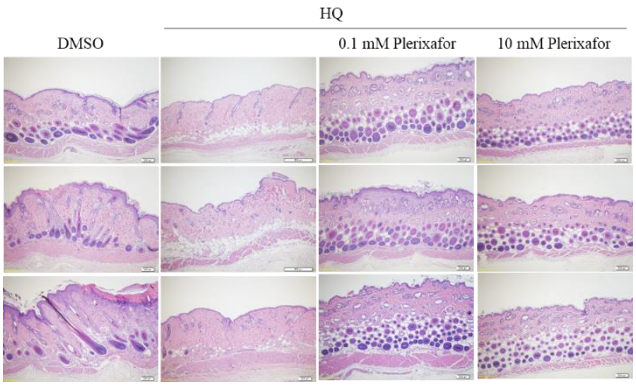

5B

 doi:10.20944/preprints202603.1777.v1

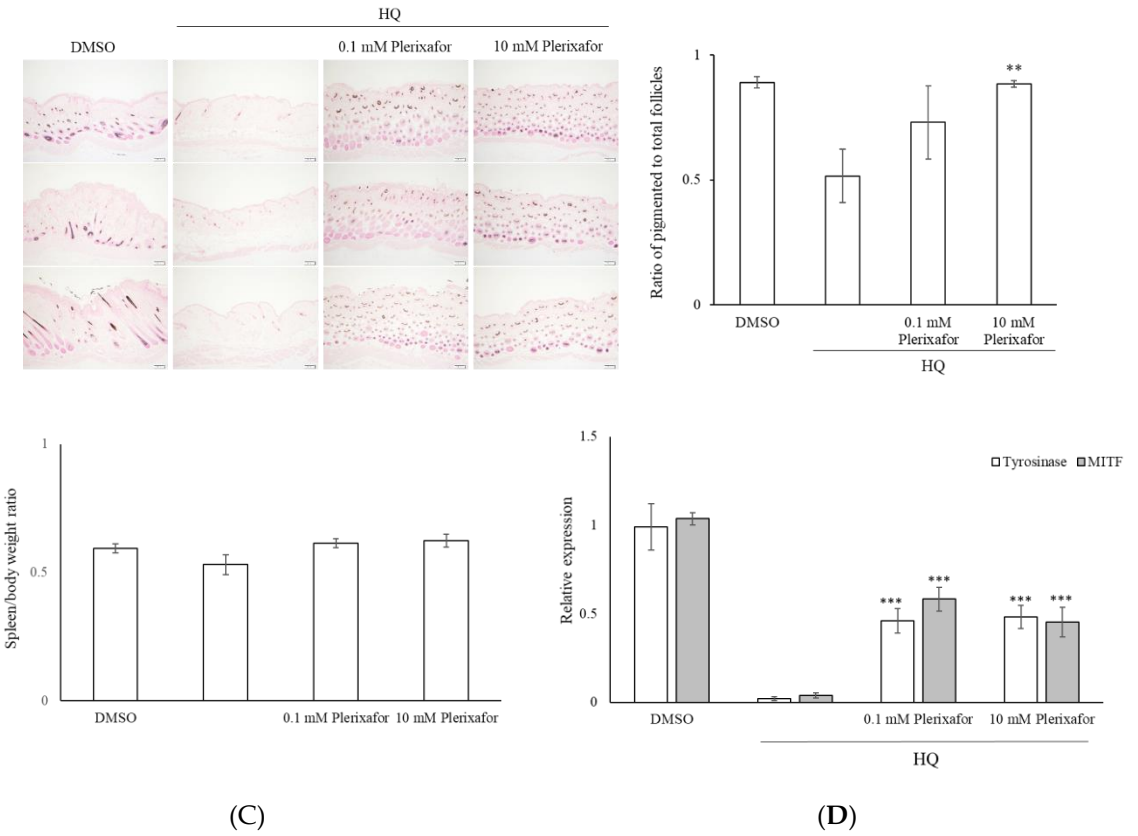

(C) (**D**)

Figure 5. Plerixafor induces re-pigmentation in HQ-treated C57BL/6 mice. (A) Represented H&E stain photographs. (B) Fontana–Masson–stained skin sections and quantified melanin content. (C) The spleen weight and body weight ratio are shown in. (D) The expression of the indicated genes in mouse skin tissue was measured by qPCR. The results are presented as the mean ± SD from three independent experiments. P-values are shown as follows: * $p < 0.05$, ** $p < 0.01$, *** $p < 0.005$ compared to the vehicle control.

Cytokine antibody array analysis demonstrated that neither HQ alone nor plerixafor, given individually or in HQ+plerixafor combination, altered the inflammatory cytokine profile compared with control. Across all 40 pro-inflammatory cytokines measured, signal intensities in the plerixafor group remained within the same range as those in the control groups, without consistent upward or downward trends, indicating that plerixafor treatment, alone or combined with HQ, did not measurably modulate this panel of inflammation-related mediators under the tested conditions (Figure 6).

Figure 6. Effect of Plerixafor on proinflammatory cytokine protein levels in the serum of mice. The cytokine expression is displayed as heatmaps, with dark green indicating no expression and red showing the highest levels observed.

 doi:10.20944/preprints202603.1777.v1

3. Discussion

CXCL12/CXCR4 represents a prototypical chemokine axis in which biased ligands can differentially engage G protein– versus β-arrestin–dependent signaling to modify cellular phenotypes. Plerixafor is clinically used as a CXCR4 antagonist for hematopoietic stem cell mobilization, but its biased actions and downstream signaling consequences in melanocytes have not been defined. Elucidating how plerixafor reprograms CXCR4 signaling at the biochemical and molecular levels, and how this translates into changes in melanocyte behavior and skin pigmentation, is therefore of interest for both GPCR biased-signaling pharmacology and drug repurposing. Our results show that plerixafor, a CXCR4 antagonist with biased signaling properties, has a strong pro-melanogenic effect by increasing MITF and tyrosinase expression in human melanocytes. The increase in MITF and tyrosinase mRNA levels after exposure to plerixafor directly supports its role in promoting melanogenic gene programs. Importantly, plerixafor countered HQ-induced suppression of melanogenesis, restoring MITF and tyrosinase expression and providing a biological rescue against depigmentation agents. It would be helpful to test the efficacy of plerixafor in combination with standard therapies (NB-UVB, topical steroids/JAK inhibitors) to determine if plerixafor enhances repigmentation in future work.

Melanocyte stem cells serve as the source of melanocyte replenishment in adult skin. They are found in specific skin niches, such as the hair follicle bulge region, the epidermal basement membrane, and sweat glands [25]. Homeostasis of melanocytes depends on the closely coordinated signaling of melanocyte stem cells, paracrine factor communication, transcriptional networks, and immune/stress responses to regulate melanocyte survival, quantity, and melanin production, thereby maintaining healthy skin pigmentation[26]. Further research is necessary to understand how recruiting these progenitor cells in specific situations can provide pigment cell sources for repigmenting depigmented areas. Yamada, T. et al. reported that CXCL12 attracts melanocyte stem cells to the proper position, facilitating the maintenance of their undifferentiated state [27]. The same team reported that differentiation of melanocytes occurs through the activation of β-catenin and migration to the epidermis to complete repigmentation in mice [28]. Our study showed that the CXCL12-CXCR4 axis antagonist plerixafor biasedly activates β-arrestin to induce β-catenin to translocate to the nucleus, interact with the T-cell-specific factor/lymphoid enhancer-binding factor 1 transcription factor (TCF/LEF-1), and bind to the TCF/LEF-1 responsive region of the MITF promoter, suggesting that plerixafor blunts the CXCL12-mediated retention signal and concomitantly terminates the undifferentiated status. Moreover, topically applied plerixafor enhances the repigmentation of depigmented skin and promotes hair follicle growth in mice, also revealing the maturation and migration of pigment cells.

β-arrestin is essential for plerixafor signaling in melanocytes as evidenced by the complete loss of plerixafor effects when β-arrestin was silenced. Plerixafor antagonizes the CXCL12-CXCR4–ERK pathway by fully blocking G-protein activation at CXCR4, while simultaneously engaging a β-arrestin-biased route that supports alternative downstream β-catenin/MITF without restoring canonical ERK signaling. This β-arrestin dependence, coupled with CXCR4 internalization, indicates that plerixafor operates via biased signaling rather than canonical G protein pathways. Future studies dissecting alternative β-arrestin–scaffolded effectors (e.g., PI3K, Src, Rho GTPases) [29] may clarify which downstream nodes drive melanogenesis versus migration. The nuclear translocation of β-catenin, observed through subcellular fractionation and ChIP-qPCR analysis, reveals a key downstream mechanism by which plerixafor boosts MITF transcriptional activity. β-catenin directly binds to the TCF/LEF motif [CTTTGAT] located near the transcriptional start site on the MITF promoter/enhancer, thereby linking CXCR4 antagonism to canonical Wnt signaling pathways that promote melanogenic gene expression. This molecular insight improves understanding of how CXCR4 signaling influences melanocyte biology beyond chemotaxis and retention.

A previously reported study revealed that CXCL12 binding to CXCR4 receptors induces the activation of integrins [30]. In essence, plerixafor's effect on cell migration was evidenced by increased motility in PIG1 cells, independent of changes in the expression of melanocyte surface

 doi:10.20944/preprints202603.1777.v1

markers c-KIT and N-cadherin. Notably, plerixafor reduced CXCR4 surface expression, consistent with prior studies showing receptor internalization driven by β-arrestin recruitment under biased antagonism. CXCR7 levels remained stable, underscoring a selective modulation of CXCR4 by plerixafor. Additionally, HQ treatment reduced the surface levels of integrin β1. It concomitantly increased integrin αv expression, consistent with a shift in available heterodimer pairs toward αv-containing receptors when β1 is limiting, as described for epithelial and carcinoma cells [22]. This pattern is compatible with altered adhesion to fibronectin-rich or vitronectin-rich matrices and, in principle, could influence melanocyte anchorage and migration. However, plerixafor did not significantly change the percentage of β1- or αv-positive cells compared with HQ alone, despite clearly enhancing transwell migration. These findings suggest that in our system, plerixafor-driven motility is predominantly mediated through CXCR4–β-arrestin signaling rather than through significant shifts in the integrin repertoire. The HQ-induced αv/β1 imbalance may sensitize melanocytes to changes in chemokine signaling [31]. Still, integrin regulation appears to play a permissive rather than primary role in the pro-migratory effects of plerixafor. Future work using integrin-blocking antibodies or defined ECM coatings will be required to dissect this crosstalk more precisely.

In our system, HQ decreased the expression of melanogenic genes, reduced CXCR4 surface levels, and altered cytoskeletal organization, thereby changing melanocyte motility, which is consistent with previous reports [32–34]. While plerixafor-induced CXCR4 downregulation can be attributed to β-arrestin-mediated receptor internalization, the mechanism underlying HQ-induced CXCR4 reduction requires further investigation, although it may involve altered receptor stability under oxidative stress. Because PIG1 cells contain little to no detectable melanin, a 2% hydroquinone solution was applied to mice to reliably induce stable hypopigmentation of the hair and skin. Given that plerixafor treatment generated round, melanin-containing hair follicles, it is inferred that plerixafor promoted hair follicle regeneration, maturation of melanogenic progenitor cells, and melanin production in both hair follicles and the epidermis. The simultaneous increase in MITF and tyrosinase gene expression in mouse skin tissue supports the in vitro results, suggesting that plerixafor promotes repigmentation by activating MITF/TYR programs in physiological settings. Additionally, the WNT/β-catenin signaling pathway is one of the earliest and most critical pathways for hair follicle induction [35]. In this study, topical plerixafor at the tested doses did not alter serum AST or creatinine levels, spleen-to-body-weight ratio, or the profile of 40 pro-inflammatory cytokines in mouse serum, suggesting a lack of overt systemic toxicity and measurable systemic inflammation under the experimental conditions. Histological examination of treated skin also did not reveal local inflammatory infiltrates or tissue damage, indicating that plerixafor's pigmentary and hair follicle effects occur without clear histopathological evidence of dermal toxicity in this model. The functional role of plerixfor related to hair follicles remains an area in need of in-depth exploration and explanation for the future.

4. Materials and Methods

4.1. Melanocyte Culture and Treatment

Human PIG1 cells (purchased from ATCC) were cultured in Dulbecco's Modified Eagle's Medium (DMEM) supplemented with 10% fetal bovine serum (Gibco; Thermo Fisher Scientific, Inc., NY, USA), 100 U/mL penicillin, and 100 μg/mL streptomycin. Maintain the cells in a humidified incubator at 37 °C with 5% CO_2. Passage cells are regularly maintained using TrypLE Express (Thermo Scientific, MA, USA) to achieve approximately 80% confluency. PIG1 cells (1×10^6/mL) were allowed to grow for 16 hours before treatment. The cells were treated with hydroquinone (1 μM) (Alfa Aesar, Thermo Fisher Scientific, MA, USA) for 8 hours, followed by the replacement with plerixafor (10 nM) (MedChemExpress, NJ, USA) for 16 hours. The non-cytotoxic and pharmacokinetic dose of 1-10 nM of plerixafor was chosen to treat cells [36]. This concentration range approximates the nanomolar plasma levels achieved clinically during stem cell mobilization and has

 doi:10.20944/preprints202603.1777.v1

been established as non-cytotoxic in primary cells, allowing mechanistic interrogation of CXCR4 biased signaling without off-target toxicity.

4.2. Cell Migration Assay

PIG1 cells were seeded at a density of 1×10^4 cells per well in the upper chamber of a Transwell plate with a pore size of 5 μm. The lower chamber contains a medium supplemented with plerixafor for 24 hours, allowing for migration. The number of migrated cells was counted under a microscope at a magnification of x200 in five random fields per well. The migration ratio was calculated as the % of trans-migrated cells compared with the DMSO vehicle control. This assay was repeated in triplicate for each experimental condition.

4.3. siRNA Transfection

β-arrestin1/2 siRNA oligonucleotides were purchased from Tri-I Biotech Inc., Taiwan. Their nucleotide sequences were as follows: β1-arrestin, 5′-AAAGCCUUCUGCGCGGAGAAU-3′ and β2-arrestin, 5′-AAGGACCGCAAAGUGUUUGUG-3′. PIG1 cells were seeded in six-well plates, and transfection was performed when the cell confluence reached approximately 60%. siRNAs (20 nM) were mixed with Lipofectamine RNAiMAX Reagent (Invitrogen, Thermo Fisher Scientific Inc.) according to the manufacturer's protocol and used for transfection. Transfection efficiency was assessed using Western blot analysis.

4.4. Flow Cytometry

PIG1 cells (1 x 10^6/ mL) were harvested and incubated with 100 ng of fluorescently conjugated monoclonal antibodies N-Cadherin (Genetex, CA, USA), c-kit (YR145; abcam), CXCR4 (HL2612; Genetex, CA, USA), CXCR7 (C1C2; Genetex, CA, USA), Integrin alpha 2 (EPR5788; abcam), Integrin alpha v (272-17E6; abcam), Integrin beta 1 (12G10; abcam) for 2 h. Cells were washed to remove unbound antibodies and then resuspended in PBS for analysis. A total of 30,000 events were recorded by the Attune NxT flow cytometer (Thermo Fisher Scientific Inc.). For each surface marker, a positive gate was established based on the control sample by setting a threshold at the mean fluorescence intensity (MFI). This gate was then applied uniformly to all treatment conditions within the same experiment. The % of positive cells was defined as the proportion of events exceeding this threshold. Data are also presented as fold change of MFI relative to vehicle controls. A minimum of three independent experiments was performed for statistical analysis.

4.5. RNA Isolation, Quantitative PCR (QPCR)

Total RNA was extracted using the TRIzol method, as per the manufacturer's instructions. The RNA was then reverse-transcribed into cDNA using the PrimeScript RT kit. The resulting cDNA was subjected to quantitative fluorescence PCR (qPCR) according to the guidelines of the SYBR Premix Ex Taq II kit (TaKaRa, Tokyo, Japan). The RT-qPCR was conducted on a 7500 instrument (Applied Biosystems, Foster City, CA, USA). The expression level was normalized against that of 18S rRNA, and the relative transcription levels were calculated using the relative quantification method ($2^{-\Delta\Delta CT}$). The primers are listed in Table S1.

4.6. Chromatin Immunoprecipitation-Quantitative PCR (ChIP-qPCR) Assay

The ChIP-qPCR assay was performed using the SimpleChIP® Plus Enzymatic Chromatin IP Kit (Cell Signaling Technology Inc.), according to the manufacturer's instructions. The cells were harvested and fixed in 1% formaldehyde with vacuum infiltration. Crosslinking was quenched by adding glycine (0.125 M). The chromatin was collected and sonicated, and then immunoprecipitated using an anti-β-catenin antibody. The immunoprecipitated DNA fragments were analyzed by quantitative PCR using specific primers (Table S2). Enriched values were normalized with the level of the IgG group.

 doi:10.20944/preprints202603.1777.v1

4.7. Western Blot Analysis

Proteins of PIG1 were immunoblotted with specific primary antibodies against ERK (1:3000; EPR17526; abcam), pERK (1:1000; EPR19401; abcam), β-catenin (1:1000; D10A8; Cell Signaling Technology, Danvers, MA, USA), β-arrestin1/2 (1:1000; D24H9; Cell Signaling Technology), β-actin (1:10000; Genetex, CA, USA), GAPDH (1:10000; Genetex, CA, USA), Lamin B1 (1:5000; Genetex, CA, USA), and then incubated with the corresponding secondary antibodies. The luminescence intensity of bands was quantified by using ImageJ.

4.8. Animals Treatments

All animal experiments were approved by the Institutional Animal Care and Use Committee of China Medical University (Approval No. CMUIACUC-2024-115) and conducted in accordance with the International Standards on Animal Welfare. Female C57BL/6 mice were purchased from the National Center for Biomodels (NCB, Taiwan). Mice were sensitized to 2% HQ by applying a DMSO solution of HQ onto shaved flanks (100 μl/mouse) for three weeks. The mice were divided into 4 groups (5 mice each) using stratified randomization. For the experimental groups, 10 mM or 0.1 mM of plerixafor was applied to the mice's backs daily for 14 days. Topical concentrations of 0.1–10 mM were selected based on preliminary dose-finding experiments and to achieve local tissue exposure sufficient for CXCR4 engagement without systemic effects. The control group received DMSO at the same interval. All mice were sacrificed and sampled on the day 37.

4.9. Specimens and Immunohistochemistry

The skin tissue (1 cm^2) of mice was harvested by administering pentobarbital (200 mg/kg, IP). The skin samples were fixed in a 4% buffered neutral formalin solution for 24 hours at room temperature, and then embedded in paraffin. Serial sections were floated in warm water containing 2% gelatin to prevent them from peeling off the sample. The 5-mm paraffin cross-sections were deparaffinized, rehydrated, and stained with hematoxylin & eosin (H&E) for histochemical analysis or with the Fontana-Masson Stain Kit for staining melanin. For each mouse, three non-overlapping fields per section were acquired from the interscapular area at 200× magnification. The image quantification was performed using ImageJ software [37]. Values from individual fields were averaged to obtain a single value per animal, and one-way ANOVA compared group means with post-hoc testing.

4.10. Inflammatory Cytokine Activity

To assess the effect of plerixfor on proinflammatory markers, the Mouse Inflammation Antibody Array - Membrane (40 Targets) (Abcam 133999, Cambridge, UK) was used, following the manufacturer's protocol. Briefly, 250 μg of serum from each sample was diluted in 1 mL of blocking buffer and applied to each array membrane. After washing, biotin-conjugated antibodies were added, followed by incubation with streptavidin conjugated to horseradish peroxidase. The membranes were then visualized with a ChemiDoc imaging system (Bio-Rad, Hercules, USA). Densitometric analysis of the signals was performed using the Protein Array Analyzer tool in ImageJ software (Research Services Branch, National Institute of Mental Health, Bethesda, USA). Array data were normalized according to the manufacturer's instructions. Heatmaps of the results were generated using Microsoft Excel.

4.11. Statistical Analysis

All quantitative data were obtained from at least three independent experiments and are presented as the mean ± standard deviation (SD). Results were statistically evaluated using one-way analysis of variance (ANOVA) followed by Tukey's post hoc test or Student's t-test, using the Statistical Package for the Social Sciences (SPSS) version 21 (IBM, Armonk, NY, USA). Significance thresholds were set at $p < 0.05$ *, $p < 0.01$ **, and $p < 0.005$ *** for comparisons with the control.

 doi:10.20944/preprints202603.1777.v1

Comparisons within the HQ group are denoted as $p < 0.05$ #, $p < 0.01$ ##, and $p < 0.005$ ### at equivalent thresholds.

5. Conclusions

In summary, this study demonstrates that plerixafor enhances melanogenesis by selectively antagonizing CXCR4 G protein signaling while recruiting β-arrestin, thereby activating β–catenin–dependent MITF transcriptional regulation. This dual mechanism promotes melanin synthesis and melanocyte migration while counteracting the effects of depigmenting agents, offering a promising strategy for therapeutic repigmentation and treatment of pigmentary disorders. Further research should investigate the interplay between integrin dynamics and CXCR4 signaling in melanocyte motility, as well as the long-term effects of plerixafor in clinical pigmentation disorders.

Supplementary Materials: The following supporting information can be downloaded at the website of this paper posted on Preprints.org.

Author Contributions: Conceptualization, Huey-Chun Huang, Tsong-Min Chang; Methodology, Tsong-Min Chang, Ting-Ya Yang; Writing, Review & Editing, Huey-Chun Huang, Tsong-Min Chang; Funding Acquisition, Huey-Chun Huang.

Funding: The Ministry of Science and Technology funded this study under grant numbers NSTC 112-2635-B-039-004 and a grant from China Medical University, Taiwan (CMU112-MF-104). We appreciate the experiments and data analysis performed through the use of the Medical Research Core Facilities Office of Research & Development at China Medical University, Taichung, Taiwan, ROC.

Conflicts of Interest: The authors declare no competing financial interests.

References

1. Snyman, M.; Walsdorf, R. E.; Wix, Sophia N.; Gill, J. G., The metabolism of melanin synthesis—From melanocytes to melanoma. **2024,** 37, (4), 438-452.
2. Sun, Q.; Lee, W.; Hu, H.; Ogawa, T.; De Leon, S.; Katehis, I.; Lim, C. H.; Takeo, M.; Cammer, M.; Taketo, M. M.; Gay, D. L.; Millar, S. E.; Ito, M., Dedifferentiation maintains melanocyte stem cells in a dynamic niche. *Nature* **2023,** 616, (7958), 774-782.
3. Kobori, C.; Takagi, R.; Yokomizo, R.; Yoshihara, S.; Mori, M.; Takahashi, H.; Javaregowda, P. K.; Akiyama, T.; Ko, M. S. H.; Kishi, K.; Umezawa, A., Functional and long-lived melanocytes from human pluripotent stem cells with transient ectopic expression of JMJD3. *Stem Cell Research & Therapy* **2023,** 14, (1), 242.
4. Coutant, K.; Magne, B.; Ferland, K.; Fuentes-Rodriguez, A.; Chancy, O.; Mitchell, A.; Germain, L.; Landreville, S., Melanocytes in regenerative medicine applications and disease modeling. *Journal of translational medicine* **2024,** 22, (1), 336.
5. Jia, X.; He, L., Unveiling the dual-edged roles of melanocytes: Key insights into skin photoaging and therapeutic avenues. *Pharmacological Research* **2025,** 218, 107848.
6. De Clercq, E., Mozobil® (Plerixafor, AMD3100), 10 years after its approval by the US Food and Drug Administration. *Antiviral chemistry & chemotherapy* **2019,** 27, 2040206619829382.
7. Jørgensen, A. S.; Daugvilaite, V.; De Filippo, K.; Berg, C.; Mavri, M.; Benned-Jensen, T.; Juzenaite, G.; Hjortø, G.; Rankin, S.; Våbenø, J.; Rosenkilde, M. M., Biased action of the CXCR4-targeting drug plerixafor is essential for its superior hematopoietic stem cell mobilization. *Communications biology* **2021,** 4, (1), 569.
8. Hira, V. V. V.; Van Noorden, C. J. F.; Molenaar, R. J., CXCR4 Antagonists as Stem Cell Mobilizers and Therapy Sensitizers for Acute Myeloid Leukemia and Glioblastoma? *Biology* **2020,** 9, (2).
9. Chen, D.; Xia, Y.; Zuo, K.; Wang, Y.; Zhang, S.; Kuang, D.; Duan, Y.; Zhao, X.; Wang, G., Crosstalk between SDF-1/CXCR4 and SDF-1/CXCR7 in cardiac stem cell migration. *Scientific Reports* **2015,** 5, (1), 16813.
10. Shi, Y.; Riese, D. J.; Shen, J., The Role of the CXCL12/CXCR4/CXCR7 Chemokine Axis in Cancer. **2020,** Volume 11 - 2020.

 doi:10.20944/preprints202603.1777.v1

11. Britton, C.; Poznansky, M. C.; Reeves, P., Polyfunctionality of the CXCR4/CXCL12 axis in health and disease: Implications for therapeutic interventions in cancer and immune-mediated diseases. **2021,** 35, (4), e21260.
12. Sison, E. A.; Magoon, D.; Li, L.; Annesley, C. E.; Rau, R. E.; Small, D.; Brown, P., Plerixafor as a chemosensitizing agent in pediatric acute lymphoblastic leukemia: efficacy and potential mechanisms of resistance to CXCR4 inhibition. *Oncotarget* **2014,** 5, (19), 8947-58.
13. Scala, S., Molecular Pathways: Targeting the CXCR4–CXCL12 Axis—Untapped Potential in the Tumor Microenvironment. *Clinical Cancer Research* **2015,** 21, (19), 4278-4285.
14. Heinrich, E. L.; Lee, W.; Lu, J.; Lowy, A. M.; Kim, J., Chemokine CXCL12 activates dual CXCR4 and CXCR7-mediated signaling pathways in pancreatic cancer cells. *Journal of translational medicine* **2012,** 10, (1), 68.
15. Nishimura, Y.; Ii, M.; Qin, G. J.; Hamada, H.; Asai, J.; Takenaka, H.; Sekiguchi, H.; Renault, M. A.; Jujo, K.; Katoh, N.; Kishimoto, S.; Ito, A.; Kamide, C.; Kenny, J.; Millay, M.; Misener, S.; Thorne, T.; Losordo, D. W., CXCR4 Antagonist AMD3100 Accelerates Impaired Wound Healing in Diabetic Mice. *Journal of Investigative Dermatology* **2012,** 132, (3), 711-720.
16. Jacquelot, N.; Duong, C. P. M.; Belz, G. T.; Zitvogel, L., Targeting Chemokines and Chemokine Receptors in Melanoma and Other Cancers. **2018,** 9.
17. Liu, H.; Liu, H.; Deng, X.; Chen, M.; Han, X.; Yan, W.; Wang, N., CXCR4 antagonist delivery on decellularized skin scaffold facilitates impaired wound healing in diabetic mice by increasing expression of SDF-1 and enhancing migration of CXCR4-positive cells. *Wound repair and regeneration : official publication of the Wound Healing Society [and] the European Tissue Repair Society* **2017,** 25, (4), 652-664.
18. Su, W.; Yu, J.; Liu, Q.; Ma, L.; Huang, Y., CXCL12/CXCR4 signaling induced itch and pain sensation in a murine model of allergic contact dermatitis. *Molecular pain* **2020,** 16, 1744806920926426.
19. Zheng, M.; Oh, S. H.; Choi, N.; Choi, Y. J.; Kim, J.; Sung, J.-H., CXCL12 inhibits hair growth through CXCR4. *Biomedicine & Pharmacotherapy* **2022,** 150, 112996.
20. McConnell, A. T.; Ellis, R.; Pathy, B.; Plummer, R.; Lovat, P. E.; O'Boyle, G., The prognostic significance and impact of the CXCR4–CXCR7–CXCL12 axis in primary cutaneous melanoma. *British Journal of Dermatology* **2016,** 175, (6), 1210-1220.
21. Searle, T.; Al-Niaimi, F.; Ali, F. R., Hydroquinone: myths and reality. *Clinical and experimental dermatology* **2021,** 46, (4), 636-640.
22. Hayashida, T.; Jones, J. C. R.; Lee, C. K.; Schnaper, H. W., Loss of beta1-integrin enhances TGF-beta1-induced collagen expression in epithelial cells via increased alphavbeta3-integrin and Rac1 activity. *J Biol Chem* **2010,** 285, (40), 30741-30751.
23. Jørgensen, A. S.; Daugvilaite, V.; De Filippo, K.; Berg, C.; Mavri, M.; Benned-Jensen, T.; Juzenaite, G.; Hjortø, G.; Rankin, S.; Våbenø, J.; Rosenkilde, M. M., Biased action of the CXCR4-targeting drug plerixafor is essential for its superior hematopoietic stem cell mobilization. *Communications biology* **2021,** 4, (1), 569.
24. Clift, I. C.; Bamidele, A. O.; Rodriguez-Ramirez, C.; Kremer, K. N.; Hedin, K. E., β-Arrestin1 and Distinct CXCR4 Structures Are Required for Stromal Derived Factor-1 to Downregulate CXCR4 Cell-Surface Levels in Neuroblastoma. *Molecular Pharmacology* **2014,** 85, (4), 542-552.
25. Huang, L.; Zuo, Y.; Li, S.; Li, C., Melanocyte stem cells in the skin: Origin, biological characteristics, homeostatic maintenance and therapeutic potential. *Clinical and translational medicine* **2024,** 14, (5), e1720.
26. Lin, J. Y.; Fisher, D. E., Melanocyte biology and skin pigmentation. *Nature* **2007,** 445, (7130), 843-50.
27. Yamada, T.; Hasegawa, S.; Hasebe, Y.; Kawagishi-Hotta, M.; Arima, M.; Iwata, Y.; Kobayashi, T.; Numata, S.; Yamamoto, N.; Nakata, S. J. A. o. D. R., CXCL12 regulates differentiation of human immature melanocyte precursors as well as their migration. **2019,** 311, (1), 55-62.
28. Yamada, T.; Hasegawa, S.; Inoue, Y.; Date, Y.; Yamamoto, N.; Mizutani, H.; Nakata, S.; Matsunaga, K.; Akamatsu, H. J. J. o. I. D., Wnt/β-catenin and kit signaling sequentially regulate melanocyte stem cell differentiation in UVB-induced epidermal pigmentation. **2013,** 133, (12), 2753-2762.
29. Miller, W. E.; Lefkowitz, R. J., Expanding roles for β-arrestins as scaffolds and adapters in GPCR signaling and trafficking. *Current Opinion in Cell Biology* **2001,** 13, (2), 139-145.

 doi:10.20944/preprints202603.1777.v1

30. Hartmann, T. N.; Burger, J. A.; Glodek, A.; Fujii, N.; Burger, M. J. O., CXCR4 chemokine receptor and integrin signaling co-operate in mediating adhesion and chemoresistance in small cell lung cancer (SCLC) cells. **2005,** 24, (27), 4462-4471.
31. Koivisto, L.; Grenman, R.; Heino, J.; Larjava, H., Integrins α5β1, αvβ1, and αvβ6 Collaborate in Squamous Carcinoma Cell Spreading and Migration on Fibronectin. *Experimental Cell Research* **2000,** 255, (1), 10-17.
32. Fabian, I. M.; Sinnathamby, E. S.; Flanagan, C. J.; Lindberg, A.; Tynes, B.; Kelkar, R. A.; Varrassi, G.; Ahmadzadeh, S.; Shekoohi, S.; Kaye, A. D., Topical Hydroquinone for Hyperpigmentation: A Narrative Review. *Cureus* **2023,** 15, (11), e48840.
33. Zang, D.; Niu, C.; Lu, X.; Aisa, H. A., A Novel Furocoumarin Derivative, 5-((diethylamino)me-13 thyl)-3-phenyl-7H-furo [3,2-g] chromen-7-one Upregulates Melanin Synthesis via the Activation of cAMP/PKA and MAPKs Signal Pathway: In Vitro and In Vivo Study. *International journal of molecular sciences* **2022,** 23, (22).
34. Inoue, Y.; Hasegawa, S.; Yamada, T.; Date, Y.; Mizutani, H.; Nakata, S.; Matsunaga, K.; Akamatsu, H., Analysis of the Effects of Hydroquinone and Arbutin on the Differentiation of Melanocytes. *Biological and Pharmaceutical Bulletin* **2013,** 36, (11), 1722-1730.
35. Ji, S.; Zhu, Z.; Sun, X.; Fu, X., Functional hair follicle regeneration: an updated review. *Signal Transduction and Targeted Therapy* **2021,** 6, (1), 66.
36. Lemery, S. J.; Hsieh, M. M.; Smith, A.; Rao, S.; Khuu, H. M.; Theresa, D.; Viano, J. M.; Cook, L.; Goodwin, R.; Boss, C.; Calandra, G.; Geller, N.; Tisdale, J.; Childs, R., A pilot study evaluating the safety and CD34+ cell mobilizing activity of escalating doses of plerixafor in healthy volunteers. **2011,** 153, (1), 66-75.
37. Schneider, C. A.; Rasband, W. S.; Eliceiri, K. W., NIH Image to ImageJ: 25 years of image analysis. *Nature Methods* **2012,** 9, (7), 671-675.